ARQII Publication
http://arqiipubl.com/ams
APPLICATIONS OF MODELLING AND SIMULATION
eISSN 2600-8084
VOL 6, 2022, 98-106

Free Vibration and Buckling Analyses of Functionally Graded Porous Columns by FEM

Lan Hoang Ton That*

Faculty of Civil Engineering, HCMC University of Architecture, Vietnam

*Corresponding author: tonthathoanglan.247@gmail.com

Submitted 22 May 2022, Revised 04 July 2022, Accepted 10 July 2022, Available online 14 July 2022.

Abstract: This article presents the free vibration and buckling behaviors of functionally graded porous (FGP) columns by using FEM (finite element method). The Matlab code developed based on the finite element formulation is validated by solving the above problems under four types of boundary condition. Numerical results which are in terms of natural frequencies and buckling load are compared with the analytical solutions and further extended to FGP columns. Besides, some mode shapes of this structure are also depicted in this article to provide specific views about the free vibration and buckling behaviors of the proposed structure.

Keywords: Buckling; Column; Finite element method; Free vibration; Functionally graded porous.

1. INTRODUCTION

Nowadays, material science has undergone great evolution, representing important fields for the development of the worlds. The introduction of the functional gradient concept in the context of composite particulate materials has contributed to the design of advanced materials able to meet specific objectives. As we all know, functional gradient materials (FGMs) were developed in Japan in the late 1980s for thermal insulation coatings [1, 2]. With more than four decades of history and being a part of a wide variety of composite materials, materials with functional gradients continue to be the object of attention. This is due to their tailorability, arising from a gradual and continuous microstructure evolution and, consequently, of locally varying material properties in one or more spatial directions. The manufacturing process is responsible for the formation of micro voids or porosities within the materials [3, 4].

Functionally graded porous (FGP) materials combine both porosity and functional gradient characteristics providing desirable properties for some applications (as in biomedical implants), and the undesirable in others where voids may cause serious problems (as in the aeronautical sector). The change in porosity in one or more directions can be caused by local density effects or pore size alteration. FGP materials possess a cell-based structure, which can be classified as open or closed (i.e., containing interconnected or isolated pores, respectively). The Young modulus and shear modulus are strongly influenced by several factors, from the manufacturing process to the size, shape, and distribution of the pores. Consequently, the analytical prediction of porous materials' properties is not simple because of the randomness present in their structures, and the need of a knowledge of the microstructure that is as accurate as possible in order to obtain a significant numerical prediction. Regarding the research object, there are many applied methods such as AM (analytical method) [5-7], FEM (finite element method) [8-12], MM (meshless method) [13, 14] to achieve the behaviors of columns. In this article, the FEM consistent with the simple beam theory is used to study the free vibration and buckling behaviors of FGP columns. Besides, a simple model helps us to reduce the computational cost with the resulting error within the allowable range.

This article has five sections. Section 1 gives the introduction as above. Section 2 presents the FGP material, section 3 shows some essential formulations as well as section 4 indicates some numerical results. Finally, a few comments are also given in section 5.

2. FGP MATERIAL

A FGP column of length L and cross section b x h is studied, where b and h are bidirectional dimensions of the column cross-section It is made by continuously changing from ceramic (c) to metal (m) phases. The volume fraction V_c of the ceramic phase follows a power-law distribution which can be written as

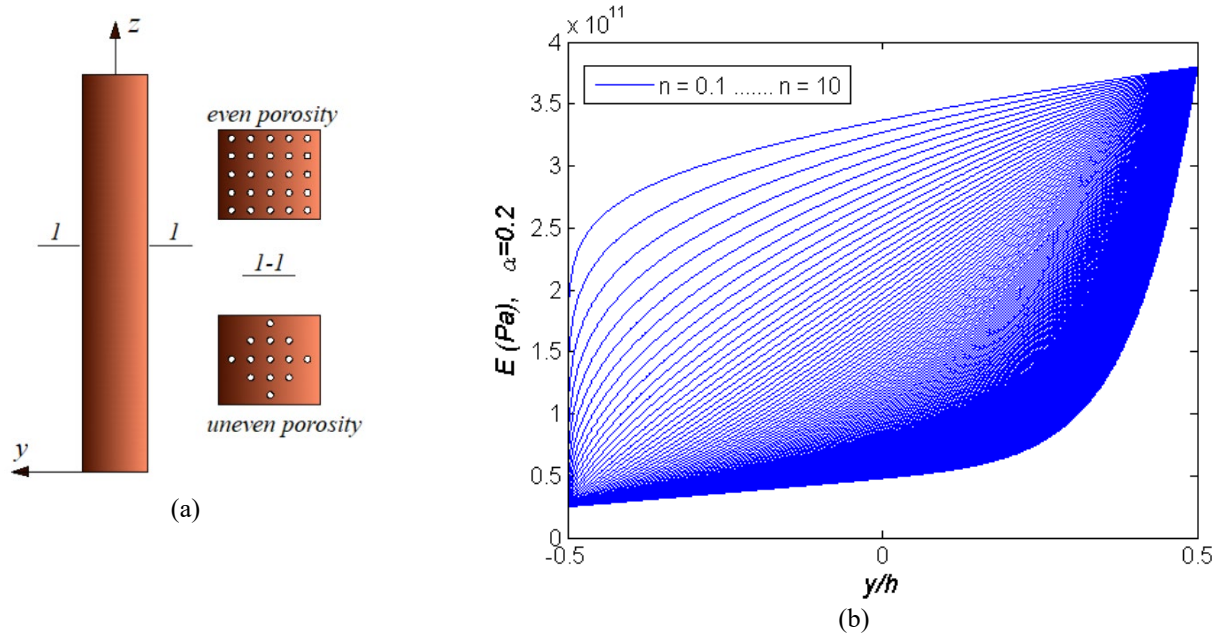

Figure 1. (a) FGP column and (b) the variation of E under even porosity with α = 0.2.

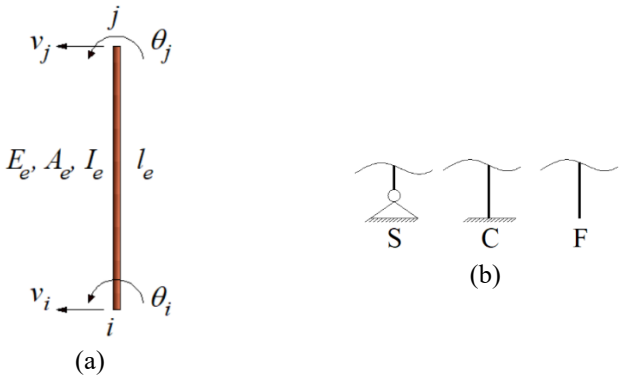

Figure 2. (a) Two-noded Euler element and (b) three boundary conditions, S (simply supported), C (clamped), F (free)

$$V_C = \left(\frac{y}{h} + 0.5\right)^n \tag{1}$$

$$V_m + V_C = 1 \tag{2}$$

where $-h/2 \leq y \leq h/2$ and n is called as the power-law index [15-17].

Due to the manufacturing process, porosities may appear as an imperfection in the functionally graded structures, leading hence to two types of porosity, namely even and uneven distributions as shown in Figure 1. The effective material properties of the FGP column are determined using the modified rule of mixture in which the porosity factor, α, $0 \leq \alpha < 1$, affects averagely the material volume fraction of each constituent,

$$P(y,\alpha) = (P_m - P_C)V_m + P_C - \frac{\alpha}{2}(P_m + P_C) \quad \text{even porosity} \tag{3}$$

$$P(y,\alpha) = (P_m - P_C)V_m + P_C - \frac{\alpha}{2}(P_m + P_C)\left(1 - 2\frac{|y|}{h}\right) \quad \text{uneven porosity} \tag{4}$$

P_m and P_C are the material properties of metal and ceramic such as Young's modulus or mass density. It can be mentioned that for even-type, the porosity phases are uniformly distributed along the column cross section, whereas for uneven-type, the porosity phases are spread mostly around the middle surface of the column cross section and vanish to the top and bottom surfaces.

3. FINITE ELEMENT FORMULATION

The column is discretized using two-noded Euler elements of length l_e with two degrees of freedom namely transverse displacement and rotation at each node as shown in Figure 2 and [9]. Moreover, E_e, A_e and I_e are Young's modulus, area of

cross section and second moment of area of element respectively.

Based on the Hermite polynomial shape functions and applying Galerkin's method, the elemental stiffness matrix can be shown as

$$\mathbf{K}_e = \frac{E_e I_e}{{I_e}^3}\begin{bmatrix} 12 & 6I_e & -12 & 6I_e \\ 6I_e & 4{I_e}^2 & -6I_e & 2{I_e}^2 \\ -12 & -6I_e & 12 & -6I_e \\ 6I_e & 2{I_e}^2 & -6I_e & 4{I_e}^2 \end{bmatrix} \tag{5}$$

In a similar way, the elemental mass matrix is presented as

$$\mathbf{M}_e = \frac{\rho A_e I_e}{420}\begin{bmatrix} 156 & 22I_e & 54 & -13I_e \\ 22I_e & 4{I_e}^2 & 13I_e & -3{I_e}^2 \\ 54 & 13I_e & 156 & -22I_e \\ -13I_e & -3{I_e}^2 & -22I_e & 4{I_e}^2 \end{bmatrix} \tag{6}$$

Finally, the elemental geometric stiffness matrix is given as

$$\mathbf{K}_{Ge} = \frac{1}{30I_e}\begin{bmatrix} 36 & 3I_e & -36 & 3I_e \\ 3I_e & 4{I_e}^2 & -3I_e & -{I_e}^2 \\ -36 & -3I_e & 36 & -3I_e \\ 3I_e & -{I_e}^2 & -3I_e & 4{I_e}^2 \end{bmatrix} \tag{7}$$

Natural frequencies ω and mode shapes can be achieved by solving the eigen value equation

$$det\left(\mathbf{K} - \omega^2 \mathbf{M}\right) = 0 \tag{8}$$

where **K** is the assembled stiffness matrix and **M** is the assembled mass matrix of column. The buckling load λ and mode shapes can also be achieved by solving the other eigen value equation

$$det\left(\mathbf{K} - \lambda \mathbf{K}_G\right) = 0 \tag{9}$$

in which $\mathbf{K}_G$ is the assembled geometric stiffness matrix of column.

4. NUMERICAL RESULTS

Firstly, an isotropic column with length L = 7 m, $b = h$ = 0.1245 m, E = 210 x 10^9 N/m^2, mass density ρ = 61.3 kg/m^3 is used to calculate natural frequencies and buckling load by using FEM. The results of this article based on 50 elements are compared with the exact solutions in references [18-20]. Tables 1 and 2 show that these numerical results converge well with the exact solutions for both free vibration and buckling analyses under four boundary conditions: CF, CC, CS and SS at two ends of the column. Figures 3 and 4 also present the first three mode shapes of column for free vibration and buckling analysis. Note that 50 elements continue to be used to study the FGP columns in the next examples.

Table 1. Comparison of the first three natural frequencies

CF	FEM (rad/s)	Exact (rad/s)	CC	FEM (rad/s)	Exact (rad/s)
Mode 1	18.7964	18.8177	Mode 1	119.6062	119.7490
Mode 2	117.7950	117.6106	Mode 2	329.6991	329.8443
Mode 3	329.8295	329.8443	Mode 3	646.3429	646.8583
CS	FEM (rad/s)	Exact (rad/s)	SS	FEM (rad/s)	Exact (rad/s)
Mode 1	82.4248	82.3274	Mode 1	52.7623	52.7644
Mode 2	267.1091	267.2968	Mode 2	211.0492	211.1645
Mode 3	557.3022	555.9774	Mode 3	474.8609	474.7192

Table 2. Comparison of buckling load under four types of boundary condition

Boundary conditions	FEM (kN)	Exact (kN)
CF	211.8088	211.8088
CC	3388.9413	3388.9226
CS	1733.2300	1733.2511
SS	847.2361	847.2497

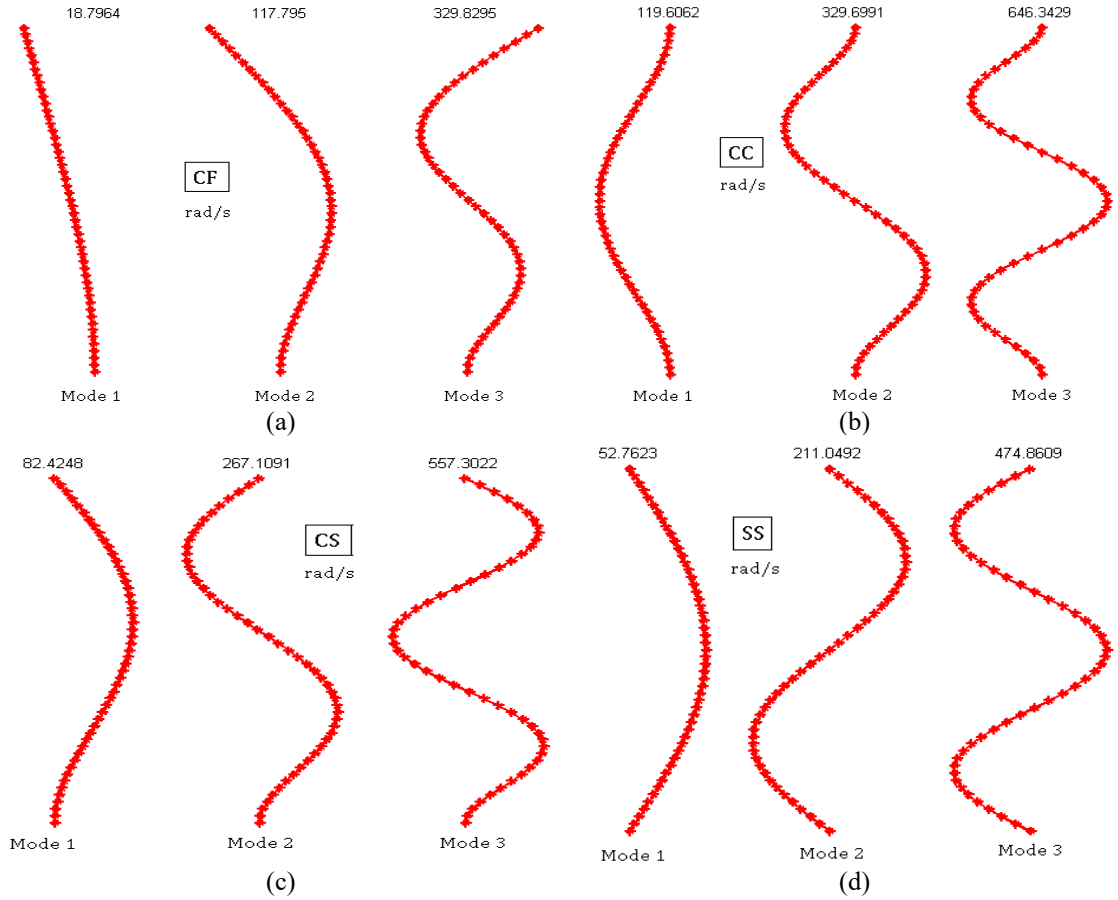

Figure 3. The first three mode shapes related to free vibration analysis

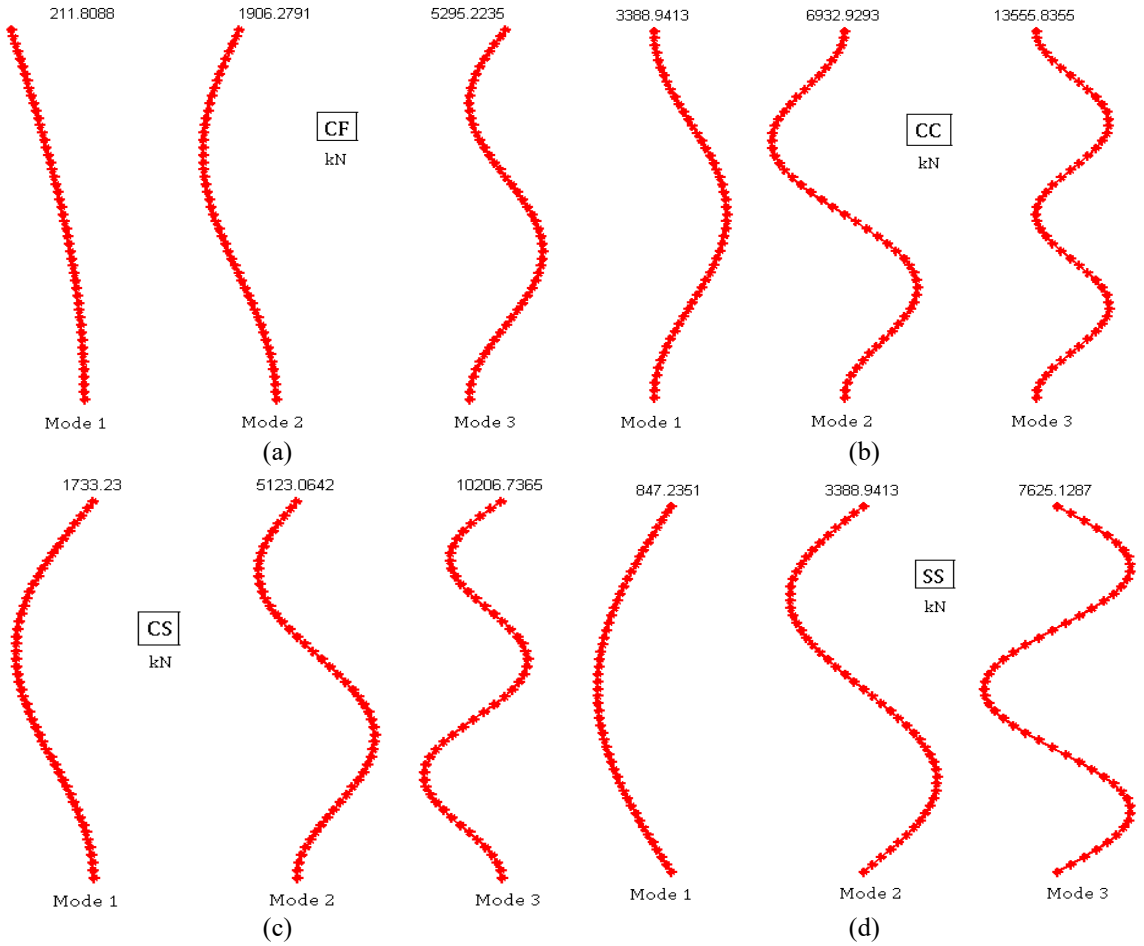

Figure 4. The first three mode shapes related to buckling analysis

Secondly, the FGP material (Al_2O_3 / Al) is applied to column with E_c = 380 GPa, ν_c = 0.3, ρ_c = 3960 kg/m^3, E_m = 70 GPa, ν_m = 0.3 and ρ_m = 2702 kg/m^3. By changing the porosity factor α, power-law index n and BCs, the first three frequencies of the column are shown in Tables 3 and 4 for both even and uneven porosities.

Table 3. The first three natural frequencies (rad/s) with type of even porosity and n = 2, 5 and 10

CF, n = 2, even porosity					
α	0.1	0.2	0.3	0.4	0.5
mode 1	2.5181	2.5013	2.4790	2.4481	2.4023
mode 2	15.7807	15.6753	15.5356	15.3419	15.0551
mode 3	44.1865	43.8912	43.5002	42.9578	42.1547
CF, n = 5, even porosity					
α	0.1	0.2	0.3	0.4	0.5
mode 1	2.3324	2.2834	2.2157	2.1157	1.9523
mode 2	14.6169	14.3101	13.8857	13.2589	12.2347
mode 3	40.9277	40.0687	38.8803	37.1253	34.2575
CF, n = 10, even porosity					
α	0.1	0.2	0.3	0.4	0.5
mode 1	2.1194	2.0271	1.8936	1.6815	1.2769
mode 2	13.2820	12.7033	11.8669	10.5378	8.0020
mode 3	37.1900	35.5696	33.2276	29.5063	22.4059
CC, n = 2, even porosity					
α	0.1	0.2	0.3	0.4	0.5
mode 1	16.0234	15.9163	15.7745	15.5778	15.2866
mode 2	44.1690	43.8739	43.4830	42.9408	42.1380
mode 3	86.5891	86.0104	85.2442	84.1813	82.6075
CC, n = 5, even porosity					
α	0.1	0.2	0.3	0.4	0.5
mode 1	14.8416	14.5301	14.0992	13.4627	12.4228
mode 2	40.9116	40.0529	38.8650	37.1106	34.2440
mode 3	80.2031	78.5197	76.1910	72.7517	67.1320
CC, n = 10, even porosity					
α	0.1	0.2	0.3	0.4	0.5
mode 1	13.4862	12.8986	12.0494	10.6999	8.1251
mode 2	37.1753	35.5556	33.2145	29.4946	22.3971
mode 3	72.8785	69.7032	65.1138	57.8213	43.9073
CS, n = 2, even porosity					
α	0.1	0.2	0.3	0.4	0.5
mode 1	11.0423	10.9685	10.8708	10.7352	10.5345
mode 2	35.7840	35.5449	35.2282	34.7889	34.1385
mode 3	74.6605	74.1616	73.5009	72.5844	71.2274
CS, n = 5, even porosity					
α	0.1	0.2	0.3	0.4	0.5
mode 1	10.2279	10.0132	9.7162	9.2776	10.5345
mode 2	33.1449	32.4492	31.4869	30.0655	34.1385
mode 3	69.1543	67.7028	65.6949	62.7294	71.2274
CS, n = 10, even porosity					
α	0.1	0.2	0.3	0.4	0.5
mode 1	9.2938	8.8889	8.3036	7.3737	5.5993
mode 2	30.1179	28.8057	26.9091	23.8954	18.1452
mode 3	62.8387	60.1009	56.1437	49.8558	37.8586
SS, n = 2, even porosity					
α	0.1	0.2	0.3	0.4	0.5
mode 1	7.0684	7.0212	6.9587	6.8719	6.7434
mode 2	28.2738	28.0848	27.8346	27.4876	26.9737
mode 3	63.6160	63.1909	62.6280	61.8471	60.6908
SS, n = 5, even porosity					
α	0.1	0.2	0.3	0.4	0.5
mode 1	6.5471	6.4097	6.2196	5.9389	5.4801
mode 2	26.1886	25.6389	24.8785	23.7555	21.9205
mode 3	58.9243	57.6876	55.9767	53.4499	49.3211

SS, n = 10, even porosity					
α	0.1	0.2	0.3	0.4	0.5
mode 1	5.9492	5.6900	5.3154	4.7201	3.5842
mode 2	23.7969	22.7601	21.2615	18.8803	14.3370
mode 3	53.5431	51.2102	47.8384	42.4807	32.2582

Table 4. The first three natural frequencies (rad/s) with type of uneven porosity and n = 2, 5 and 10

CF, n = 2, uneven porosity					
α	0.1	0.2	0.3	0.4	0.5
mode 1	2.5636	2.5994	2.6391	2.6835	2.7335
mode 2	16.0660	16.2900	16.5390	16.8172	17.1303
mode 3	44.9852	45.6126	46.3096	47.0886	47.9654
CF, n = 5, uneven porosity					
α	0.1	0.2	0.3	0.4	0.5
mode 1	2.3966	2.4269	2.4609	2.4994	2.5433
mode 2	15.0193	15.2091	15.4223	15.6635	15.9389
mode 3	42.0544	42.5859	43.1829	43.8584	44.6294
CF, n = 10, uneven porosity					
α	0.1	0.2	0.3	0.4	0.5
mode 1	2.2059	2.2268	2.2506	2.2776	2.3089
mode 2	13.8241	13.9554	14.1040	14.2738	14.4695
mode 3	38.7079	39.0755	39.4917	39.9670	40.5150
CC, n = 2, uneven porosity					
α	0.1	0.2	0.3	0.4	0.5
mode 1	16.3130	16.5405	16.7932	17.0757	17.3937
mode 2	44.9674	45.5946	46.2913	47.0700	47.9465
mode 3	88.1541	89.3837	90.7495	92.2761	93.9944
CC, n = 5, uneven porosity					
α	0.1	0.2	0.3	0.4	0.5
mode 1	15.2502	15.4429	15.6594	15.9044	16.1840
mode 2	42.0377	42.5691	43.1658	43.8411	44.6117
mode 3	82.4109	83.4525	84.6224	85.9461	87.4569
CC, n = 10, uneven porosity					
α	0.1	0.2	0.3	0.4	0.5
mode 1	14.0367	14.1699	14.3209	14.4932	14.6920
mode 2	38.6926	39.0600	39.4761	39.9512	40.4990
mode 3	75.8531	76.5734	77.3890	78.3204	79.3943
CS, n = 2, uneven porosity					
α	0.1	0.2	0.3	0.4	0.5
mode 1	11.2418	11.3986	11.5728	11.7675	11.9866
mode 2	36.4308	36.9389	37.5033	38.1342	38.8443
mode 3	76.0100	77.0701	78.2478	79.5640	81.0456
CS, n = 5, uneven porosity					
α	0.1	0.2	0.3	0.4	0.5
mode 1	10.5094	10.6423	10.7914	10.9603	11.1529
mode 2	34.0573	34.4878	34.9712	35.5183	36.1426
mode 3	71.0579	71.9560	72.9647	74.1061	75.4088
CS, n = 10, uneven porosity					
α	0.1	0.2	0.3	0.4	0.5
mode 1	9.6731	9.7650	9.8690	9.9878	10.1247
mode 2	31.3472	31.6449	31.9819	32.3668	32.8107
mode 3	65.4035	66.0246	66.7278	67.5309	68.4569
SS, n = 2, uneven porosity					
α	0.1	0.2	0.3	0.4	0.5
mode 1	7.1962	7.2966	7.4081	7.5327	7.6730
mode 2	28.7848	29.1863	29.6323	30.1307	30.6918
mode 3	64.7659	65.6692	66.6726	67.7942	69.0566

SS, n = 5, uneven porosity					
α	0.1	0.2	0.3	0.4	0.5
mode 1	6.7274	6.8124	6.9079	7.0160	7.1393
mode 2	26.9095	27.2496	27.6316	28.0638	28.5571
mode 3	60.5463	61.3116	62.1711	63.1437	64.2536
SS, n = 10, uneven porosity					
α	0.1	0.2	0.3	0.4	0.5
mode 1	6.1920	6.2508	6.3174	6.3935	6.4811
mode 2	24.7682	25.0034	25.2697	25.5738	25.9245
mode 3	55.7284	56.2576	56.8568	57.5411	58.3301

The different porosity distributions affect the magnitude of the material characteristic values and thereby affect the resulting vibration as well as the stability of the structure. In the case of even porosity, the value of the first frequency decreases when the porosity factor α increases, but in the case of uneven porosity, the value of this frequency increases when the porosity factor increases, as shown in Figures 5 and 6. As the porosity factor increases in the case of uneven porosity, the stiffness matrix **K** and mass matrix **M** change with the tendency to increase the achieved eigenvalue in Equation 8, respectively. Furthermore, in both cases, we get the maximum value of the natural frequency corresponding to the CC boundary condition, then a decrease from CS to SS and finally, the smallest value for the CF boundary condition.

Finally, the buckling load with two types of porosity can be achieved in this study by using FEM. Table 5 and Figure 7 give the specific values for buckling load under four kinds of boundary condition: CF, CC, CS and SS, n = 1 and 15 and α = 0.1, 0.2, 0.3 and 0.4. As the porosity increases, the buckling load decreases for all cases of change, respectively.

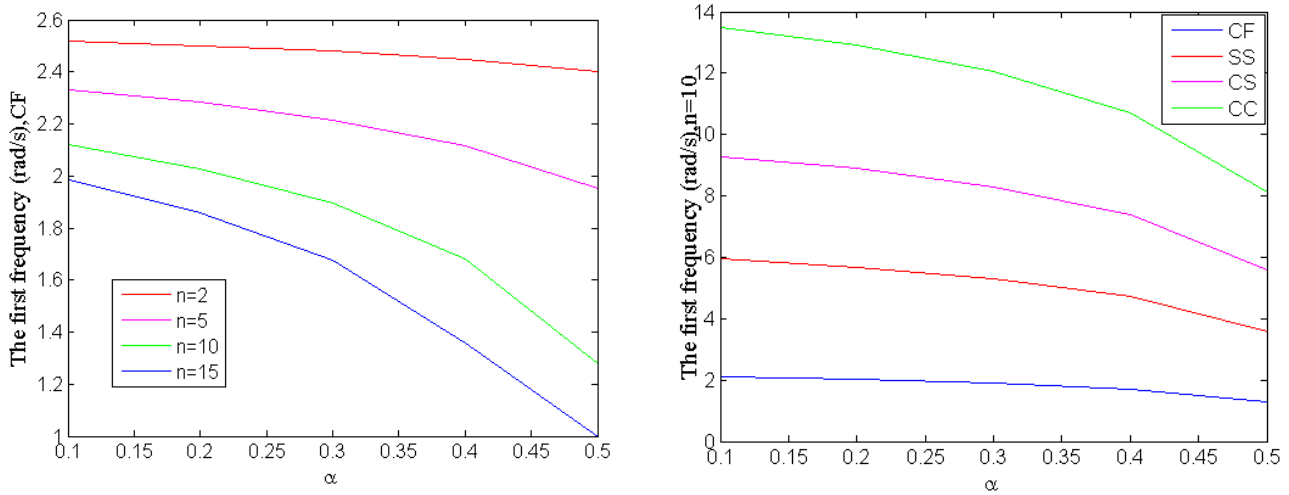

(a) The first frequency by changing n (b) The first frequency by changing BCs

Figure 5. Variation of the first natural frequency of the FGP column under even porosity

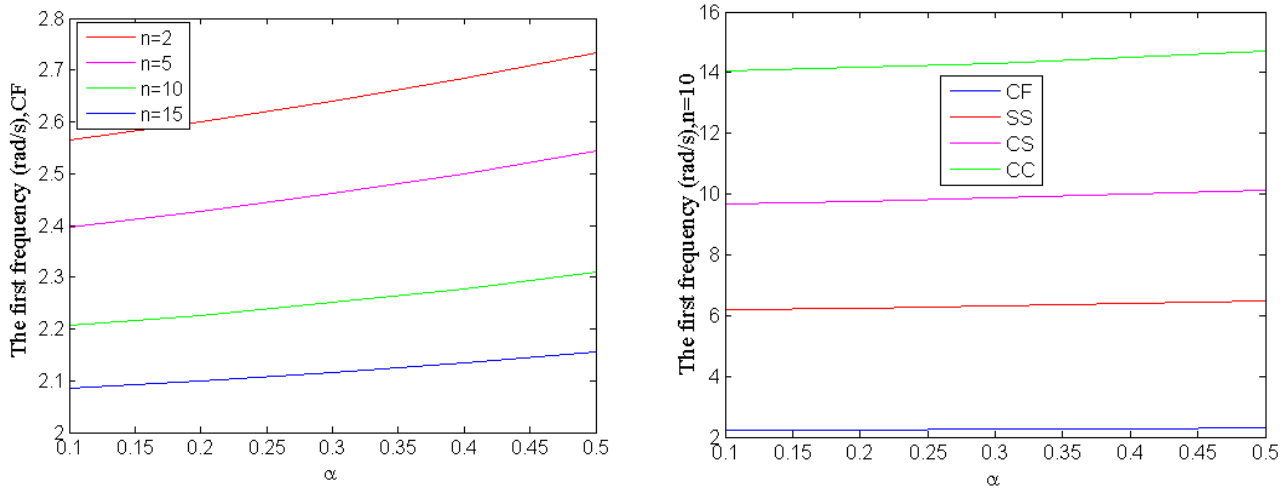

(a) The first frequency by changing n (b) The first frequency by changing BCs

Figure 6. Variation of the first natural frequency of the FGP column under uneven porosity

Table 5. The buckling load (kN) with two types of porosity, n = 1 and 15, and α = 0.1, 0.2, 0.3 and 0.4

		Even porosity			
n	α	CF	CC	CS	SS
1	0.1	204.2	3266.6	1670.7	816.6
	0.2	181.5	2903.6	1485.0	725.9
	0.3	158.8	2540.7	1299.4	635.2
	0.4	136.1	2177.7	1113.8	544.4
		Uneven porosity			
n	α	CF	CC	CS	SS
1	0.1	221.2	3538.8	1809.9	884.7
	0.2	215.5	3448.1	1763.5	862.0
	0.3	209.8	3357.3	1717.1	839.3
	0.4	204.2	3266.6	1670.7	816.7
		Even porosity			
n	α	CF	CC	CS	SS
15	0.1	94.2	1507.8	771.1	377.0
	0.2	71.6	1144.9	585.5	286.2
	0.3	48.9	781.9	399.9	195.5
	0.4	26.2	418.9	214.3	104.7
		Uneven porosity			
n	α	CF	CC	CS	SS
15	0.1	111.3	1780.0	910.4	445.0
	0.2	105.6	1689.3	864.0	422.3
	0.3	99.9	1598.6	817.6	399.6
	0.4	94.2	1507.8	771.2	377.0

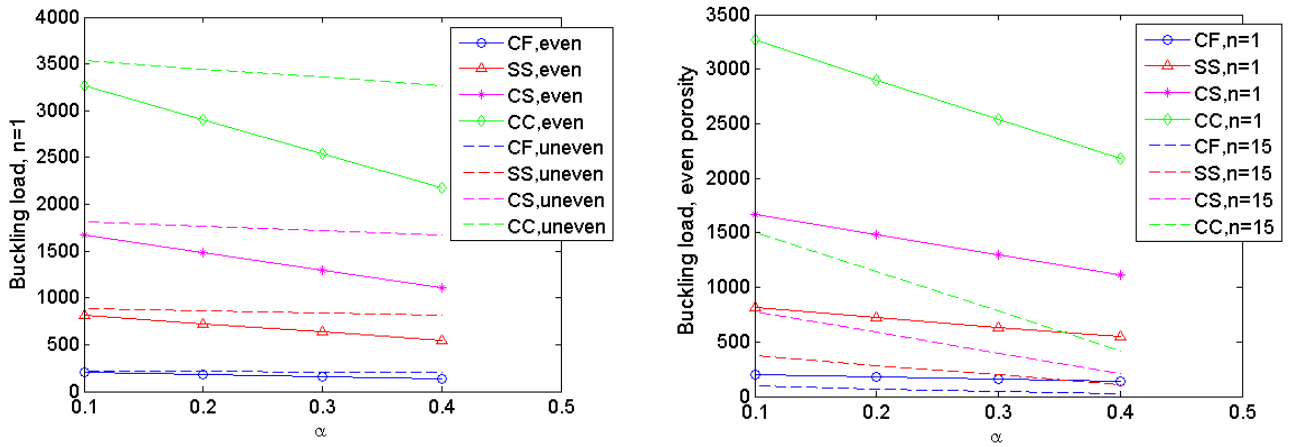

(a) Buckling load with n = 1 (b) Buckling load with even porosity

Figure 7. Variation of the buckling load (kN) of the FGP column

5. CONCLUSION

This work presents the free vibration and buckling behaviors of FGP columns under several boundary conditions and two types of porosity by using FEM. The results of this article are good and agree well with exact solutions for isotropic material. Besides, the main aim of this paper is to develop the applicability of two-noded Euler elements to analyzing the FGP columns with acceptable results. The results drawn from this article will contribute to guide future in-depth analysis related to this type of structure.

ACKNOWLEDGMENT

No funding.

REFERENCES

[1] R. M. Mahamood and E.T. Akinlabi, *Functionally Graded Materials*. Springer International Publishing, 2017.
[2] K. Ichikawa, *Functionally Graded Materials in the 21st Century: A Workshop on Trends and Forecasts*. Springer USA, 2001.
[3] A. Öchsner, G. E. Murch and M. J. S. de Lemos, *Cellular and Porous Materials: Thermal Properties Simulation and Prediction.* Wiley, 2008.

[4] Z. Liu, *Multiphysics in Porous Materials*. Springer International Publishing, 2018.
[5] B. Akgöz and Ö. Civalek, A size-dependent shear deformation beam model based on the strain gradient elasticity theory, *International Journal of Engineering Science*, 70, 2013, 1-14.
[6] M. Şimşek and J. N. Reddy, Bending and vibration of functionally graded microbeams using a new higher order beam theory and the modified couple stress theory, *International Journal of Engineering Science*, 64, 2013, 37-53.
[7] M. Şimşek and H. H. Yurtcu, Analytical solutions for bending and buckling of functionally graded nanobeams based on the nonlocal Timoshenko beam theory, *Composite Structures*, 97, 2013, 378-386.
[8] D. S. Mashat, E. Carrera, A. M. Zenkour, S. A. Al Khateeb and M. Filippi, Free vibration of FGM layered beams by various theories and finite elements, *Composites Part B: Engineering*, 59, 2014, 269-278.
[9] S. S. Kolukula, Available from: https://sites.google.com/site/kolukulasivasrinivas/.
[10] D. -Q. Vo, and H. L. Ton-That, Free vibration of simply supported steel I-girders with trapezoidal web corrugations, *Reports in Mechanical Engineering*, 1(1), 2020, 141-150.
[11] H. L. Ton-That, Plate structural analysis based on a double interpolation element with arbitrary meshing, *Acta Mechanica et Automatica*, 15(2), 2021, 91-99.
[12] M. J. Aubad, S. O. W. Khafaji, M. T. Hussein and M. A. Al-Shujairi, Modal analysis and transient response of axially functionally graded (AFG) beam using finite element method. *Materials Research Express*, 6(10), 2019, 10654.
[13] Y. Yang, C. C. Lam, K. P. Kou and V. P. Iu, Free vibration analysis of the functionally graded sandwich beams by a meshfree boundary-domain integral equation method, *Composite Structures*, 117, 2014, 32-39.
[14] M. Chehel Amirani, S. M. R. Khalili and N. Nemati, Free vibration analysis of sandwich beam with FG core using the element free Galerkin method, *Composite Structures*, 90(3), 2009, 373-379.
[15] N. T. Giang, Free vibration exploration of rotating FGM porosity beams under axial load considering the initial geometrical imperfection, *Mathematical Problems in Engineering*, 2021, 5519946.
[16] H. L. That Ton, A study of functionally graded porous beam based on simple beam theory, *International Journal of Engineering and Applied Physics*, 1(3), 2021, 226-234.
[17] L. H. That Ton, Effect of porosity on free vibration of functionally graded porous beam based on simple beam theory *Technical Journal of Daukeyev University*, 2(1), 2022, 1-10.
[18] L. H. Donnell, *Beams, Plates and Shells*. McGraw-Hill, 1976.
[19] S. Timoshenko, *Strength of Materials: Elementary Theory and Problems*, R. E. Krieger Publishing Company, 1976.
[20] S. Timoshenko, *Theory of Elasticity*, McGraw-Hill Education (India), 2010.